Polymer 51 (2010) 5604–5611

Contents lists available at ScienceDirect

Polymer

journal homepage: www.elsevier.com/locate/polymer

Deformation-induced phase transitions of polyamide 12 in its elastomer segmented copolymers

Liangui Bai [a], Zhihua Hong [b], Daoliang Wang [a], Junjun Li [a], Xiao Wang [a], Guoqiang Pan [a], Liangbin Li [a,b,*], Xiuhong Li [c]

[a] National Synchrotron Radiation Lab and College of Nuclear Science and Technology, University of Science and Technology of China, Hefei, China
[b] CAS Key Lab of Softmatter Chemistry, University of Science and Technology of China, Hefei, China
[c] Shanghai Synchrotron Light Facility, Shanghai, China

ARTICLE INFO

Article history:
Received 19 June 2010
Received in revised form
11 September 2010
Accepted 15 September 2010
Available online 29 September 2010

Keywords:
PTHF–PA12
α″ phase
Tensile

ABSTRACT

Deformation-induced phase transition behavior of polyamide 12 (PA12) in its segmented copolymers with polytetrahydrofuran (PTHF) was studied with in-situ wide angle X-ray scattering (WAXS) at different temperatures. In these segmented copolymers, which contain a high content of PTHF, a transformation from the stable γ phase to a metastable α″ phase is observed during tensile deformation at room temperature, which shows a similar diffraction behavior to that of the α phase but without an obvious melting point. The deformation-induced α″ phase is not a thermodynamic stable phase but arises from kinetic origins, which is in line with the condition for its formation. After the release of tensile force following deformation, the metastable α″ phase can partially transform back to the initial γ phase. The reversible phase nature may contribute somewhat to the elasticity of PTHF–PA12 systems as a result of this enthalpic contribution. Upon increasing the content of PTHF in the copolymer, the critical stress required to induce the new α″ phase increases. Upon increasing strain, the α″ phase will disappear in the samples that possess a particularly high content of PA12. Higher temperatures also prevent the γ phase from transforming to the α″ phase.

1. Introduction

Thermoplastic elastomers (TPEs) are copolymers segregated into hard and soft domains, which are superior both in their processing and recycling in comparison with vulcanizates and received extensive interest in academy and polymer industry [1–13]. The hard domains are either glassy or crystalline at room temperature, whereas the soft domains are usually in the rubbery state which endure major deformation. Deformation-induced crystallization of the soft domains is of importance on the mechanical performance, which may enhance the strength and toughness like that in natural rubber. Thus great effort has been dedicated to the deformation-induced crystallization of the soft segments [1–5]. For example, deformation-induced crystallization of poly(tetramethylene oxide) (PTMO) and polyethylene oxide (PEO) has been observed in a wide range of copolymers with them as soft segments and polyamide as hard segments, where a critical strain is generally required to induce crystallization [4].

During tensile deformation, the hard domains of TPEs are normally assumed to being intact as they are defined as "hard". This is partially true as the tensile stress is rather low, comparing to the stress required to deform the homopolymer of the hard segments. However, a simple comparison of the tensile stresses on copolymer and homopolymer is not reliable to justify whether the hard segments undergo structural change or not during tensile deformation. The mechanical properties depend primarily on the domain sizes, the volume ratio between the soft and the hard domains, and the connectivity of the hard phase [14–16]. Incorporating the soft segments may affect crystallinity, crystal size and superstructure of the hard domains. For example, in segmented copolymers PTMO–polyamide 12 (PTMO–PA12) or polytetrahydrofuran–PA12 (PTHF–PA12), the presence of the soft segments reduces the crystal size and crystallinity of the PA12 hard domains, which has a lower melting temperature and stability than those of the homopolymer. High content of soft segments can even prevent PA12 from forming spherulitic superstructures. Thus it is expected that crystal–crystal transitions of PA12 in the copolymers require a lower stress than that in the homopolymer. In this case, deformation-induced crystal–crystal transitions may also contribute

* Corresponding author. National Synchrotron Radiation Lab and College of Nuclear Science and Technology, University of Science and Technology of China, Hefei, China. Tel.: +86 0551 3602081.
E-mail address: lbli@ustc.edu.cn (L. Li).

0032-3861/$ – see front matter © 2010 Elsevier Ltd. All rights reserved.
doi:10.1016/j.polymer.2010.09.038

to the mechanical properties through an enthalpic fashion instead of only the rubber entropy from the soft segments.

In this work, commercial segmented copolymers PTHF–PA12 from Evonik Degussa are used as a model system to study the structural evolution during tensile deformation. Deformation-induced crystal–crystal phase transitions are common behaviors of polyamide. PA12 has four different crystal phases denoted α, γ, α' and γ' forms depending on the crystallization conditions [17–20]. The γ form is the most common form with a hexagonal or sometimes pseudo hexagonal packing, which is characterized with a strong diffraction peak with d spacing around 0.41–0.42 nm [21]. The α form belongs to monoclinic system [21–23], which gives two strong diffraction peaks with d spacings of about 0.37 and 0.45 nm. The crystal structure consists of hydrogen bonded sheets with fully extended and antiparallel chains. The α form can be obtained under the following conditions: crystallization or casting from solution [24], drawing just below the melting point [25], and crystallization under high pressure above 500 MPa [26]. The α' phase can be observed near the melting temperature of PA12, characterized by two diffraction peaks in wide angle X-ray scattering (WAXS), which are closer to each other than those of the α phase [19]. The γ' form has a similar WAXS pattern as that of γ form, which can transform to α phase through thermal treatment under pressure. The same thermal treatment does not transform the γ form into the α crystal [17,26]. External fields induced transitions among the four crystal phases of PA12 homopolymer have been systematically studied before [17,24–35]. With in-situ WAXS, recently our group studied the deformation-induced phase transition of PA12 at different temperatures, where a transient phase is observed in the plastic deformation region during tensile deformation [27]. Segmented copolymer of PTHF and PA12 is TPEs in which PTHF segments act as soft rubber component and PA12 hard domains play a role as physical cross-links. Here we extend our early work to study the effect of PTHF content on the deformation-induced phase transitions of PA12 with in-situ WAXS. During tensile deformation, the transient phase in homopolymer PA12 is found to be kinetically stable in the copolymers with high content of PTHF, whose life time decreases with the increase of either temperature or the content of PA12.

2. Experimental section

2.1. Material and sample preparation

PTHF–PA12 granules with series ratios of PA12/PTHF were kindly supplied by Evonik Degussa with a trade name of VESTAMID and used after being dried in a vacuum oven at 50 °C for 24 h. PTHF–PA12 plates with a thickness about 1 mm were obtained through compression molding. The granules were first melted at 220 °C for 15 min, and then cooled down to room temperature within 30 min. For tensile testing, the plates were cut into dog-bone shaped samples with length and width of 24 and 4 mm, respectively.

The contents of PTHF and PA12 were measured by proton nuclear magnetic resonance (NMR) using trifluoroacetic acid-d_1 (TFA-d_1) as solvent and lock. Three reference peaks were extracted to calculate the molar ratio of the two segments. The reference peaks were the methylene peaks next to the oxygen on PTHF at *ca.* 3.76 ppm, next to the nitrogen of PA12 at *ca.* 3.58 ppm, and next to the carboxyl of the adipic acid at *ca.* 2.75 ppm. Based on the molar ratio we obtained the mass ratio, which is presented in Table 1.

2.2. Tensile tests and structure measurements

The dog-bone shaped samples were mounted between two clamps of a homemade miniature tensile tester, which is equipped with a temperature controlled oven with nitrogen purge. The drawing speed was fixed at 5.8 μm/s. The initial length of the samples between two clamps was about 17 mm. The change of sample width was followed with a high-precision CCD camera. Uniaxial tensile tests were performed at several designated temperatures.

Table 1
Mass ratio of PA12/PTHF as determined via ^{1}H NMR.

Sample name	E50	E60	E80	E100
PA12/PTHF	49/51	58/42	82/18	100/0

In-situ WAXS measurements were carried out on the synchrotron radiation X-ray scattering station with a radiation wavelength of 0.154 nm and Mar345 image plate as a detector in National Synchrotron Radiation Laboratory (NSRL) in Hefei (China). Fit2D software package was used to analyze the two-dimensional (2D) WAXS patterns. Small angle X-ray scattering (SAXS) was performed on the station in Shanghai Synchrotron Radiation Facility (SSRF). The SAXS patterns were recorded on Mar165 CCD camera with a sample to detector distance of 1.87 m. The wavelength λ is 0.124 nm.

Differential scanning calorimetry (DSC) thermograms were measured on a Shimadzu DSC-60 instrument. Fourier transformation infrared (FTIR) absorption measurements were carried out on a Nicolet 8700 instrument. The thin films with a thickness of about 100 μm were prepared with a microtome at room temperature. Laser Raman spectra were obtained with a LABRAM-HR (JY, France) laser Raman Spectroscope equipped with a microscope. The excitation wavelength is 514.5 nm with an Argon ion laser.

3. Results

The crystal phase in the PA12 segmented copolymer samples before tensile test in this work was the γ phase, which was verified by the WAXS pattern. Two main WAXS peaks were observed at 2θ of about 21.5° and 5.8°, which correspond to (001) and (020) diffractions of the γ phase of PA12, respectively.

Fig. 1a depicts the true stress–strain curve of E50 during tensile test at room temperature (25 °C controlled by air condition), where selected 2D WAXS patterns at various strain levels are inserted. The brighter color means greater intensity. There are two shoulder peaks before stretching. The broad one at low angle side is from amorphous principally due to PTHF phase. The one at large angle side is due to γ phase. The development of deformation-induced orientation of crystals can be easily visualized through 2D WAXS patterns. After deformation, two obvious diffraction arcs show up in the meridianal direction of the 2D WAXS patterns. To obtain detailed information, integrated one-dimensional (1D) WAXS curves are given in Fig. 1b. The diffraction intensity is collected from the meridianal direction within the azimuthal angle range of 70°–110°, which covers the main oriented arcs induced by deformation. As shown in Fig. 1b, before deformation there is a peak at 2θ of 21.5°, identified as $(001)_\gamma$ diffraction of the γ phase. The intensity of $(001)_\gamma$ peak decreases with the increase of true strain and stress. When the true stress reaches a critical value, two new diffraction peaks appear, whose intensities increase with strain. These two peaks locate at the small and large angle sides of the $(001)_\gamma$, respectively. The critical true stress for the occurrence of the new diffraction peaks is about 13.1 MPa. At high strain, the γ phase also exists according to the diffraction peak of (020). The amount of the γ phase decreases, which makes the $(001)\,\gamma$ less obvious. In order to estimate the exact position of the two new peaks, 1D WAXS curves of the sample with true strains of 0 and 2.5 are shown in Fig. 1c,

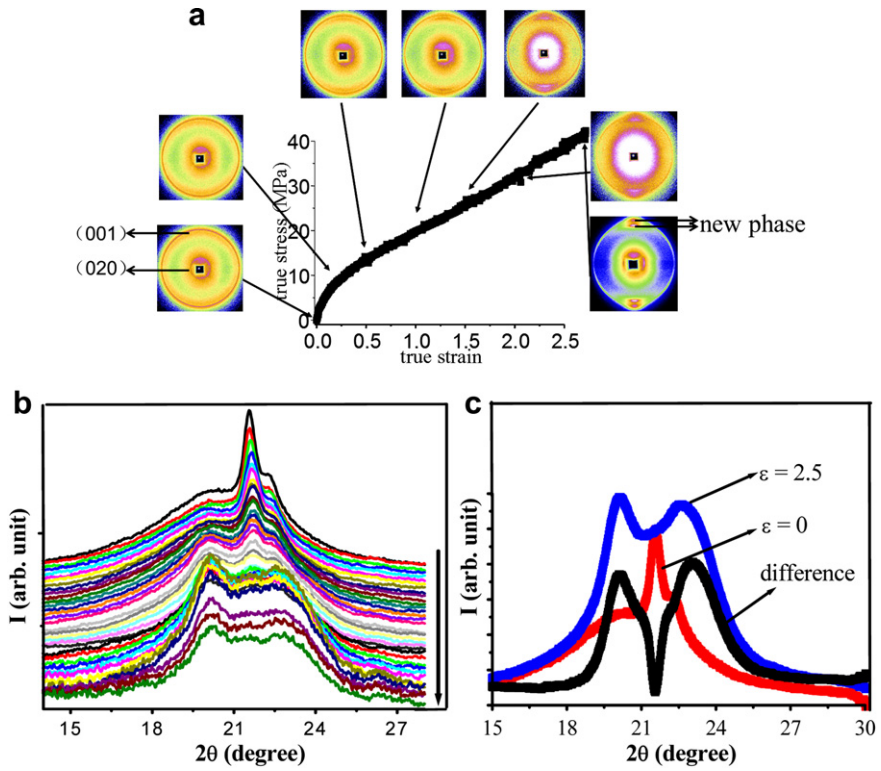

Fig. 1. True stress–strain curve and the selected 2D WAXS patterns during tensile test of E50 at room temperature (a) (Tensile direction is along the horizontal direction). Integrated one-dimensional WAXS curves in the meridianal direction (b). The arrow indicates the increase of strain. The WAXS curves of samples with true strain ε of 0, 2.5 and their difference (c).

where the difference between them is also displayed. Peak fitting shows the positions of the two new peaks at 2θ of about 20.1° (d = 0.441 nm) and 23.4° (d = 0.379 nm), respectively, which are close to the expected diffraction of the α phase of PA12. The appearance of PTHF crystal is excluded as its main diffraction peak at 2θ of 24.7° is not observed. Thus tensile deformation induces the formation of a new crystal phase of PA12, which has similar diffractions as the α phase.

In order to further identify the deformation-induced new phase, its thermal behavior, IR and Raman spectra were investigated. Fig. 2 gives DSC curves of the undeformed and the deformed E50 samples with true strain ε of 2.5. The DSC data further confirm the absence of PTHF crystal in the copolymer. The DSC with a heating rate of 90 °C/min is also done, which has a similar result to that with a low heating rate. Fig. 3 shows the IR spectra of the deformed (ε = 2.5) and the undeformed samples. No absorption band of the PTHF crystal phase appears in both the deformed and the undeformed samples. Taking the symmetric stretching mode of the ester C=O group at 1737 cm^{-1} as a reference for PA12, the absorption band (shoulder peak) at 677 cm^{-1} (amide V of α; C=O out of plane) is observed in the deformed sample, which indicates that the new deformation-induced phase has a similar structure as that of the α form of PA12. Fig. 4 shows the Raman spectra of the deformed (ε = 2.5) and the undeformed samples. The 1111 cm^{-1} peak is from the trans C–C symmetric conformation of the γ phase in the undeformed sample. Both the shift of this peak to 1123 cm^{-1} and the increase of 1470 cm^{-1} peak ′ intensity in the deformed sample (ε = 2.5) indicates that α type crystal is induced by tensile deformation. [36]. However, we cannot directly assign this deformation-induced phase as the α crystal since the α crystal in homopolymer PA12 forms under deformation at temperature close the melting point of PA12.

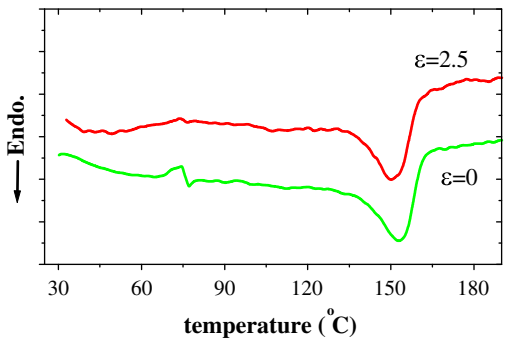

Fig. 2. DSC heating scans of the undeformed and the deformed E50 films.

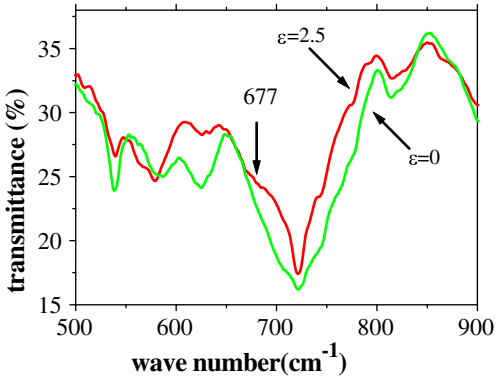

Fig. 3. IR spectra of the undeformed and the deformed E50 film.

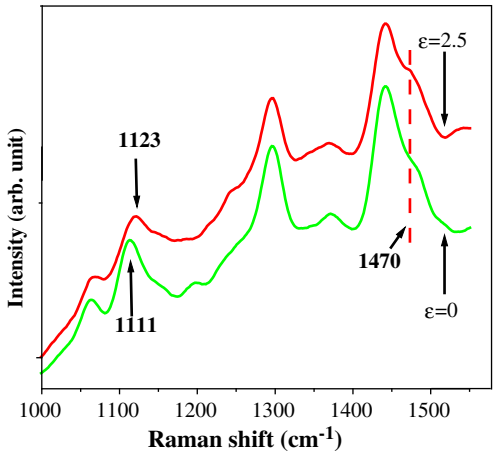

Fig. 4. Raman spectra of the undeformed and the deformed E50 film.

As DSC measurement of the deformed sample only gives one single melting peak, which shows no obvious difference from the undeformed sample, we employed in-situ WAXS measurements to track the melting behavior of the deformation-induced new phase. The 1D diffraction curves of the deformed sample during heating scan are presented in Fig. 5a. The temperature range of the heating scan is from room temperature (25 °C) to 190 °C with a rate of 1 °C/min. The diffraction peaks of the deformation-induced new phase locate at 2θ of 19.7° and 23.4° (identified with difference method), while the (001) peak of the γ phase locates at 2θ of 21.4°. Upon increasing temperature, the intensity of the diffraction peaks of the deformation-induced new phase decreases. At 74 °C, the peaks of the deformation-induced new phase disappear completely. In order to have a close look at the phase transition behavior of the new phase, the diffraction intensity of the peak at 19.7° during heating scan is plotted in Fig. 5b, which decreases linearly with the temperature. No obvious melting or discontinuous transition of the new phase is observed, which is consistent with the DSC result. On the other hand, the content of the γ phase increases during heating, which suggests that a transition from the new phase to the γ phase in melting and re-crystallization takes place. The results from the heating scan reveal that the deformation-induced new phase is not a thermodynamic stable phase but arises from kinetic origins. This is understandable as it is induced under a non-thermodynamic circumstance. External work from deformation and temperature affords the activation energy for phase transitions. Without the aid of external work, the thermal activation energy alone cannot induce such transition. For convenience, the deformation-induced new phase is labeled as α″ phase.

In order to check the possible recovery of the new phase, the cooling experiment was also done from 105 °C to room temperature. Note even with zero load on the samples, both the crystal and amorphous region keep partially orientation before completely melting, as revealed by in-situ WAXS measurements. As shown in Fig. 5c, the diffraction peaks of the deformation-induced α″ phase appear again at 72 °C during cooling, located at 2θ of 19.8° and 23.4°. Upon cooling to room temperature, the intensity of these diffractions increases. Only part of the initial α″ phase recovered. It is supported by the result that the two peaks' diffraction intensities after cooling to room temperature are lower than that before heating. (see Fig. 5d). In order to check the temperature memory effect, we also did the experiment heated to higher temperature.

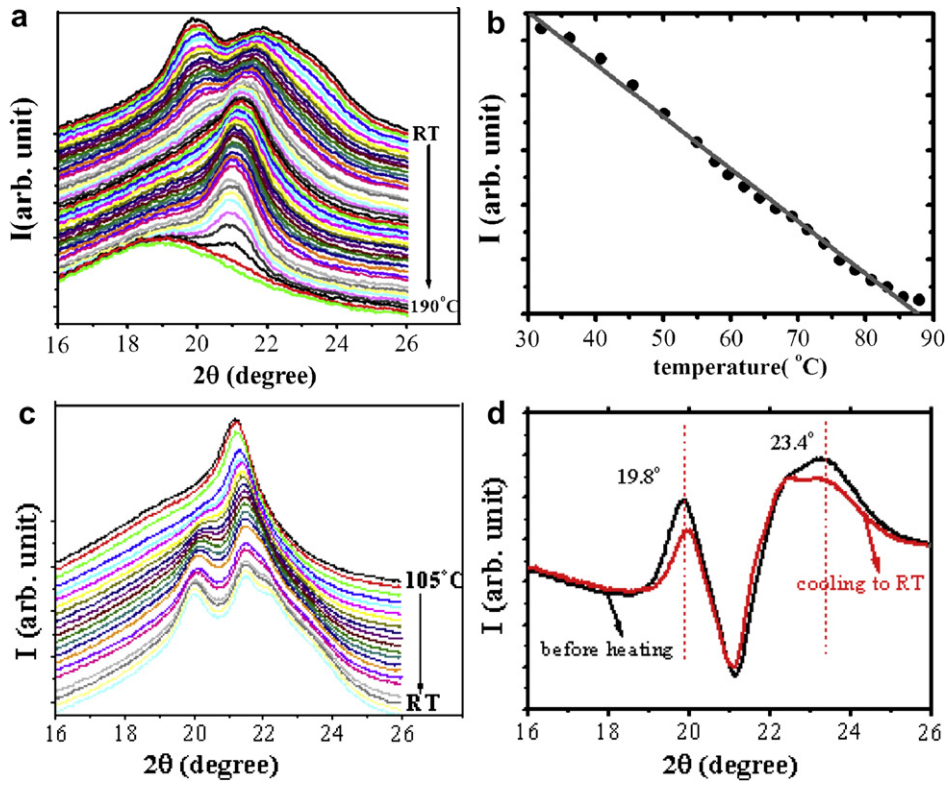

Fig. 5. X-ray diffraction curves of the deformed E50 film ($\varepsilon = 2.5$) obtained during heating scan from room temperature to melting (a) and the corresponding intensity evolution of the peak at 19.7° (b). X-ray diffraction curves of the deformed E50 film obtained during cooling scan from 105 °C to room temperature (c), difference figures of sample before heating and cooling to RT (d).

The higher temperature the deformed sample heated, the smaller the content of α″ phase recovered when cooled to room temperature. Accompanying the recovery of the α″ phase during cooling, the intensity of the amorphous halo decreases. This suggests that the α″ phase crystallizes from the oriented amorphous phase rather than transforms from the γ phase, as the orientation of the amorphous phase still partially remains after the disappearance of the α″ phase at high temperature. Higher final heat-up temperature erases more memory of amorphous orientation, which leads to less recovery of the α″ phase. As under zero load the γ phase is more stable than the α″, and thus it is not possible for the γ phase to transform back to the α″ phase.

Due to its kinetic origin, it is natural to expect that the α″ phase of PA12 in E50 may transform back to the γ phase upon releasing the stress even at room temperature. In order to check this possibility, cyclic experiments were conducted on the E50 sample. Fig. 6a shows the true stress–stain curve. Fig. 6b and c depict the structural evolution in the first and second cycles, respectively. In zone I, the sample is undergoing tensile deformation process. When the true stress increases to a critical value of 12 MPa, the α″ phase forms. In zone II, the load is removed with a retraction speed of 5.8 μm/s, the content of the α″ phase decreases. After removing the force completely, the α″ phase still exists. The structural evolution in the second cycle is similar to that in the first one. Fig. 6d shows the comparison between the samples at true strain ε of 2.7 and after completely removing the load. Obviously, the content of the α″ phase reduces after removing the stress while the γ phase increases. The results from the cyclic experiments indicate that the deformation-induced α″ phase can partially transform back to the initial γ phase even at room temperature.

The temperature dependence on the deformation-induced phase transition is further studied at 60, 80 and 100 °C. As shown in Fig. 7a, when the E50 sample was stretched at 60 °C, the structure evolution is similar with that at 25 °C. The $(001)_\gamma$ peak is originally at 2θ of 21.5°. New diffraction peaks at 2θ of 20.3° and 23° appear during tensile deformation. The critical true stress for the formation of the α″ phase at 60 °C is 7.38 MPa, which is lower than that at 25 °C (13.1 MPa). When the temperature is even higher, the structure evolution is different from that at lower temperatures. Fig. 7b and c depict the structural evolution of samples during tensile deformation at 80 and 100 °C, respectively. The initial main diffraction peak is still at 2θ of 21.5°, but the two new diffraction peaks occurred at low temperatures do not appear during tensile deformation at high temperatures. The final samples after tensile deformation give a broad scattering halo, which indicates a deformation-induced disordering takes place at high temperatures.

The effect of PTHF content on the deformation-induced phase behavior is further studied on a series of PTHF–PA12 segmented copolymers with different ratios of PA12/PTHF. Fig. 8a presents the true stress–strain curve and selected 2D WAXS patterns of E60 during tensile test at room temperature, which has a ratio between PA12 and PTHF of 58/42. The structural evolution behavior of E60 is closely similar to that of E50. As shown in Fig. 8b, the two characteristic diffraction peaks of the α″ phase appear during tensile deformation. The critical true stress for the formation of the α″ phase in E60 is 20.7 MPa, which is much larger than that of E50 (13.1 MPa). Further increasing the content of PA12, the structural evolution follows a different fashion during tensile deformation at room temperature, though deformation can still induce the α″ phase in these samples. For conciseness, we only present the 1D WAXS curves for E80 and E100 in Fig. 8c and d, respectively. The peaks of the α″ phase of E80 and E100 is difficult to distinguish with naked eyes, especially in E100, where the α″ phase is just a transient phase. The difference WAXS curve for the true strain at $\varepsilon = 0.4$

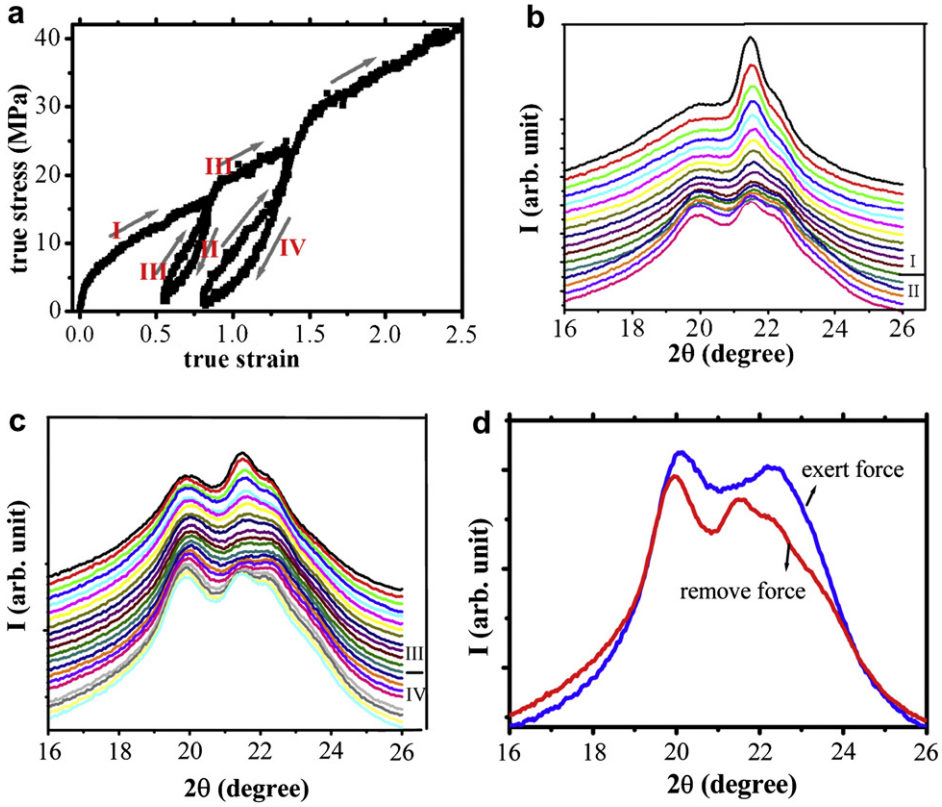

Fig. 6. Tensile true stress–strain curve of E50 at room temperature (a). Arrows indicate the direction of deformation. X-ray diffraction intensity curves collected from meridianal scans at first cycle (b), second cycle (c), comparison of the WAXS curves of sample exerted and removed force (d).

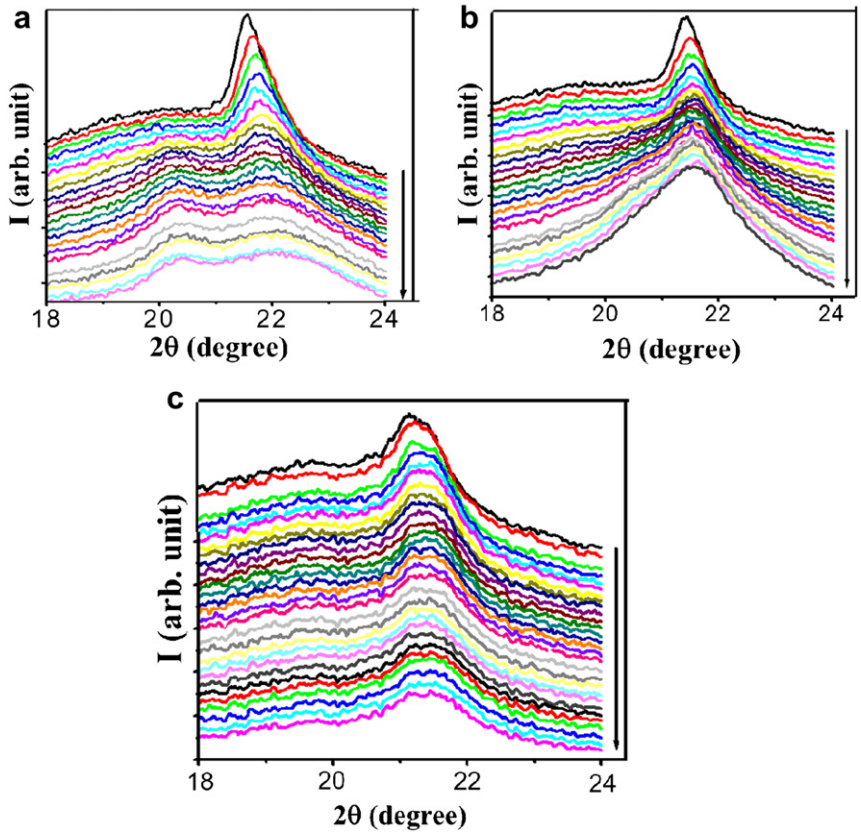

Fig. 7. X-ray diffraction intensity curves collected from meridianal scans while stretching E50 at 60 °C (a), 80 °C (b), 100 °C (c).

and $\varepsilon = 0$ from E80 is shown in Fig. 8e, which makes the two peaks of the α'' phase more visible. The critical true stresses for the formation of the α'' phase in E80 and E100 are 36.7 MPa and 55.3 MPa, respectively. This result indicates that the critical true stress for the formation of the α'' phase increases with the content of PA12. Further increasing the strain, the signal of these peaks disappears gradually and a broad scattering halo is observed in the final deformed samples. The complete disappearance of the α'' phase in homopolymer PA12 (E100) occurs at a true stress of 60.9 MPa. This suggests that the α'' phase only survives within a specific stress range. Thus with a high content of PA12, the α'' phase is a transient phase during tensile deformation.

Fig. 9 gives the evolution of the (020) d spacing (d_{020}) of PA12 and PTHF–PA12 segmented copolymers during tensile deformation at 25 °C. The d_{020} of homopolymer PA12 (E100) decreases firstly to a minimum and then increases sharply, which is similar to another study within our group [27]. The d_{020} follows a different behavior in PTHF–PA12 segmented copolymers. In E80, the d_{020} decreases first to a plateau and then increases slightly in the final stage. The d_{020} of E50 and E60 only slightly decrease to a plateau value during tensile test. If the transition from the initial γ phase to the final state follows a direct process, one would expect the evolution of the d_{020} spacing would behavior in a monotonic fashion. This does occur on E50 and E60, where a transition from the initial γ phase to the final α'' phase takes place. The new diffraction peaks of deformed E50 and E60 prove the transition from the γ phase to the α'' phase definitely. The evolution of the d_{020} spacing in E80 and E100 is non-monotonic and has a minimum with strain. This further confirms that the α'' form is only a transient phase during the transition from the initial γ structure to the final structure in samples with high contents of PA12.

4. Discussion

In-situ WAXS measurements during tensile deformation of PTHF–PA12 segmented copolymers give two conclusions. (i) A metastable α'' phase is induced through tensile deformation, which can only survive within a specific stress window. (ii) The deformation-induced α'' phase is kinetically stable, which can partially transform back to the stable γ phase after releasing the stress or increasing temperature.

Without stress, we have a thermodynamic stability sequence of $\gamma > \gamma\prime > \alpha\prime\prime$ at high temperatures. Imposing stress switches the relative stability of those phases, which leads to the initial metastable α'' phase to being stable. External work from deformation and temperature afford the activation energy for molecular segments to overcome the free energy barriers for phase transitions. Without the aid of external work, the thermal activation energy alone cannot induce such transitions. Stress and temperature provide an activation energy enough to transform γ phase to the α'' phase. At room temperature, the contribution of temperature is small on the activation energy as without external stress the transition from the γ to the α'' phases does not occur at all. Moreover the glass transition temperature of homopolymer PA12 (about 40 °C) is higher than room temperature. Thus the activation energy to overcome the energy barrier is mainly from tensile stress. Further increasing either stress or temperature turns the stable α'' phase again into metastable one, which transforms correspondingly into either the mesomorphic state at room temperature or the γ' phase at high temperatures.

As for the most common thermoplastic elastomers, the elastic properties originate from a reversible conformational transition. Unlike the most common elastomers, PTHF–PA12 is a semi-

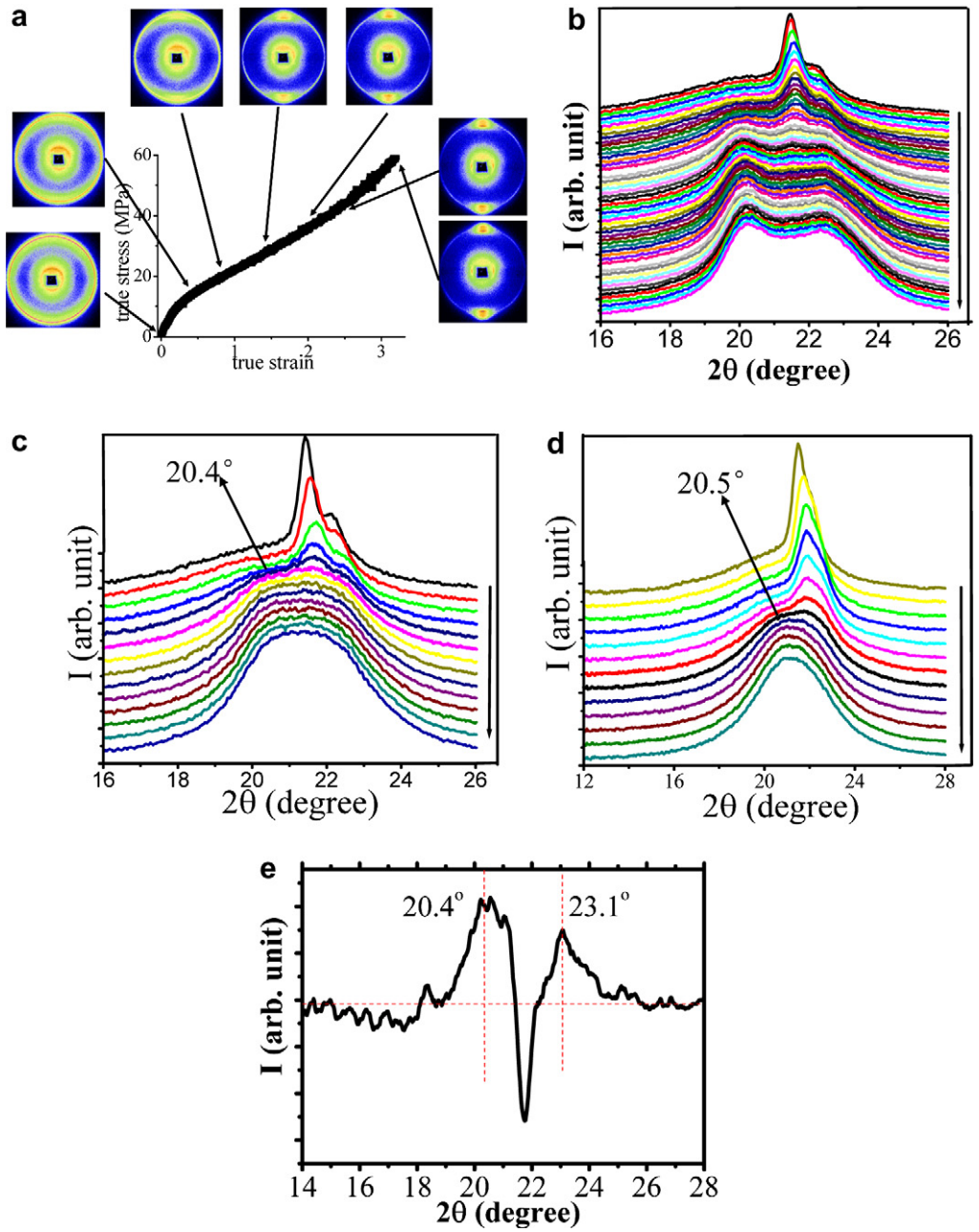

Fig. 8. True stress–strain curve and the selected 2D WAXS patterns of E60 during tensile test at room temperature (a), corresponding 1D curves collected from meridianal direction (b). 1D WAXS curves collected from meridianal directions of E80 (c) and E100 (d) during tensile test, respectively. Difference WAXS curves of E80 (e) (The right arrow indicates the increase of strain).

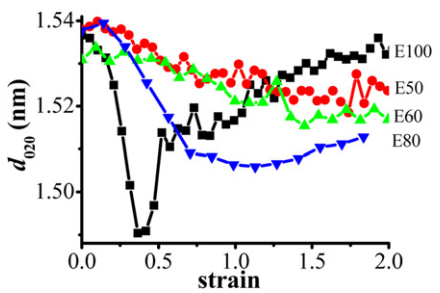

Fig. 9. Evolution of (020) *d* spacing of PTHF–PA12 segmented copolymers during tensile deformation at 25 °C.

crystalline material, and the conformational transition occurs in both the crystalline and the amorphous regions. During the mechanical cycles at room temperature, the soft segment PTHF is in the rubber state, which undergoes a reversible conformational transition from random coil to stretched state without the occurrence of crystallization. Meanwhile in the crystalline region, deformation-induced phase transitions happen in the PA12 hard domains. Upon reaching a critical stress, the stable γ phase transforms to the metastable α″ phase. After the release of load, the reversible transition from the metastable α″ phase back to the γ phase occurs. This crystal transition takes place during the relaxation of the material and is probably partly responsible for elasticity of the material. It can contribute to the mechanical property through an enthalpic fashion instead of only the rubber entropy from the soft segments [37–41].

5. Conclusion

The structural evolution of segmented copolymer PTHF–PA12 during tensile deformation was studied with in-situ WAXD. Upon reaching a critical stress, the stable γ phase transforms into a metastable α'' phase, which shows a similar diffraction behavior with that of the α phase but without an obvious melting point. After the release of load, partially reversible transition from the metastable α'' phase back to the γ phase occurs. The elasticity of the PTHF–PA12 TPEs may be partly due to this crystal transition through enthalpic fashion instead of only rubber entropy from the soft segment. With low content of PTHF soft segment, the α'' phase is a transient phase in the transition from the initial γ phase to the final state, which survives only within a specific range stress window. During tensile deformation increasing either the content of PA12 or temperature has a negative effect on the life time of the α'' phase.

Acknowledgments

L.B. Li would like to thank Dr Zhidong Chen (Degussa) for providing PA12 sample. This work is supported by the NNSFC (20774091, 50973103, 50903089), 973 program (2010CB934504), fund for one hundred talent scientist of CAS and the experimental fund of NSRL and SSRF. The research is also in part supported by the Opening Project of the State Key Laboratory of Polymer Materials Engineering (Sichuan University KF201001).

References

[1] Tashiro K, Hiramatsu M, Kobayashi M, Tasokoro H. Sen-1 Gakkaishi 1986; 42:597–605.
[2] Hatfield GR, Guo Y, Killinger WE, Andrejak RA, Roubicek PM. Macromolecules 1993;26:6350–3.
[3] Song YH, Yamamoto H, Nemoto N. Macromolecules 2004;37:6219–26.
[4] Sheth JP, Xu J, Wilkes GL. Polymer 2003;44:743–56.
[5] Liu LZ, Yeh F, Benjamin C. Macromolecules 1996;29:5336–45.
[6] Konyukhova EV, Buzin AI, Godovsky YK. Thermochim Acta 2002;391:271–7.
[7] Floudas G, Tsutsilianis C. Macromolecules 1997;30:4381–90.
[8] Liu LZ, Jiang B. J Polym Sci B Polym Phys 1998;36:2961–70.
[9] Benjamin C, Liu LZ. J Polym Sci B Polym Phys 1999;37:779–92.
[10] Hucher C, Eustache RP, Beaume F, Tekely P. Macromolecules 2005;38:9200–9.
[11] Boulares A, Tessier M, Maréchal E. Polymer 2000;41:3561–80.
[12] Drozdov AD. Polymer 2006;47:3650–60.
[13] Hatfield GR, Bush RW, Killinger WE. Polymer 1994;35:3943–7.
[14] Krishnaswamy RK, Yang Q, Ballester LF, Kornfield JA. Macromolecules 2008;41:1693–704.
[15] Janzen J. Polymer Eng Sci 1992;32:1242–54.
[16] Janzen J. Polymer Eng Sci 1992;32:1255–60.
[17] Hiramatsu N, Haraguchi K, Hirakawa S. Jpn J Appl Phys 1983;22:335–9.
[18] Mathias LJ, Johnson CG. Macromolecules 1991;24:6114–22.
[19] Jones NA, Atkins EDT, Hill MT, Cooper SJ, Franco L. Polymer 1997;38:2689.
[20] Li LB, Koch MHJ, de Jeu WH. Macromolecules 2003;36:1626–32.
[21] Aharoni SM. n-Nylons: their synthesis, structure and properties. Chichester: John Wiley & Sons; 1997 [Chapter 1.3].
[22] Cojazzi G, Fichera A, Garbuglio C, Malta V, Zannetti R. Makromol Chem 1973;168:289–301.
[23] Holmes DR, Bunn CW, Smith DJ. J Polym Sci 1955;17:159–77.
[24] Ishikawa T, Nagai S, Kasai N. J Polymer Sci Polymer Phys Ed 1980;18:1413–9.
[25] Ishikawa T, Nagai S, Kasai N. Makromol Chem 1981;182:977–88.
[26] Stamhuis JE, Pennings AJ. Polymer 1977;18:667–74.
[27] Wang DL, Shao CG, Zhao BJ, Bai LG, Wang X, Li LB. Macromolecules 2010;43:2406–12.
[28] Northolt MG, Tabor BJ, van Aartsen JJ. J Polymer Sci 2 Polymer Phys 1972; 10:191–2.
[29] Czarnecki MA, Wu P, Siesler HW. Chem Phys Lett 1998;283:326–32.
[30] Dencheva N, Nunes TG, Oliveira MJ, Dencheva Z. J Polym Sci B Polym Phys 2005;43:3720–33.
[31] Dencheva N, Denchev Z, Oliveira JM, Nunes TG, Funari SS. J Appl Polym Sci 2008;109:288–302.
[32] Ozaki Y, Liu YL. Macromolecules 1997;30:2391–9.
[33] Rhee S, White JL. J Polym Sci B Polym Phys 2002;40:1189–200.
[34] Ishikawa T, Nagai S. J Polym Sci Polym Phys Ed 1977;15:1315–7.
[35] Ishikawa T, Nagai S, Kasai N. Makromol Chem 1979;180:2999–3001.
[36] Stephens JS, Chase DB, Rabolt JF. Macromolecules 2004;37:877–81.
[37] Auriemma F, de Balleateros OR, De Rosa C. Macromolecules 2001;34:4485–91.
[38] Auriemma F, De Rosa C, Espostio S, Mitchell GR. Angew Chem Int Ed Engl 2007;46:4325–8.
[39] De Rosa C, Auriemma F, Corradi M, Caliano L, Talarico G. Macromolecules 2008;41:8712–20.
[40] Auriemma F, De Rosa C. Macromolecules 2003;36:9396–410.
[41] De Rosa C, Auriemma F, Corradi M, Caliano L, de Balleateros OR, Girolamo RD. Macromolecules 2009;42:4728–38.